Odovtos-International Journal of Dental Sciences (Odovtos-Int. J. Dent. Sc.), Online First, 2025. ISSN: 2215-3411
https://doi.org/10.15517/m983tw41

ODOVTOS
International Journal of Dental Sciences

UNIVERSIDAD DE COSTA RICA FOd Facultad de Odontología

https://revistas.ucr.ac.cr/index.php/Odontos

BASIC RESEARCH:

The Histone Deacetylase Inhibitor Sodium Butyrate Stimulates Adipogenesis Through a Limited Transcriptional Switch in Periodontal Ligament-Derived Stem Cells

El inhibidor de la histona desacetilasa butirato de sodio estimula la adipogénesis a través de un cambio transcripcional limitado en células troncales derivadas de ligamento periodontal

Anahí Torres-Nájera[1-2] https://orcid.org/0009-0006-0845-0024
Angélica Anahí Serralta-Interían[1-2] https://orcid.org/0000-0003-2062-2141
Rodrigo Arturo Rivera-Solís[1] https://orcid.org/0000-0002-5721-9615
Geovanny Nic-Can[3] https://orcid.org/0000-0001-8003-7716
Leydi Carrillo-Cocom[1] https://orcid.org/0000-0002-5477-7603
Beatriz Adriana Rodas-Junco[2-3] https://orcid.org/0000-0002-2804-6073

[1]Facultad de Ingeniería Química, Universidad Autónoma de Yucatán, Inn, Perif. de Mérida Lic. Manuel Berzunza 13615, Chuburná de Hidalgo. C.P. 97203, Mérida, Yucatán, México.
[2]Laboratorio de Células Troncales-Facultad de Odontología, Universidad Autónoma de Yucatán, Calle 61-AX Av. Itzaés Costado Sur "Parque de la Paz", Col. Centro. C.P. 97000, Mérida, Yucatán, México.
[3]SECIHTI-Facultad de Ingeniería Química, Universidad Autónoma de Yucatán, Periférico Norte Kilómetro 33.5, Tablaje Catastral 13615, Chuburná de Hidalgo Inn. C.P. 97203, Mérida, Yucatán, México.

Correspondence to: Beatriz Adriana Rodas-Junco - beatriz.rodas@correo.uady.mx

Received:4-II-2025 Accepted: 9-VII-2025

ABSTRACT: Adipogenic differentiation plays a crucial role in adipose tissue biology, an endocrine organ that regulates energy storage and hormone secretion. Dysfunction in this process contributes to metabolic diseases such as obesity and type II diabetes. In vitro models have been developed to investigate the mechanisms of adipogenesis, with periodontal ligament stem cells (PDLSCs) emerging as a promising model due to their multipotent capacity. Previous studies have shown that epigenetic manipulation can enhance the adipogenic response in various cell lines. Acetylation of lysine 9 on histone H3 (H3K9ac) is associated with the activation of key genes, such as PPARγ-2. In this study, we evaluated whether class I histone deacetylase inhibitors, such as valproic acid (VPA) and sodium butyrate (NaBu), both short-chain fatty acids, can increase H3K9 acetylation and influence adipogenic differentiation. We used 1, 4, and 8 mM VPA concentrations and 1, 2, and 5 mM NaBu to assess their effects on cell viability, morphology, H3K9ac distribution, and adipogenic differentiation. The results indicated that cells treated with 5 mM NaBu exhibited morphological changes, reduced viability, increased H3K9ac signal intensity, and enhanced intracellular lipid deposition. These results infer that inhibition of HDACs by NaBu increases plasticity toward adipogenesis of PDLSCs through a limited transcriptional change in their key genes.

KEYWORDS: Periodontal ligament stem cells; Histone acetylation; Adipogenesis; Histone deacetylase inhibitors.

RESUMEN: La diferenciación adipogénica desempeña un papel crucial en la biología del tejido adiposo, un órgano endocrino que regula el almacenamiento de energía y la secreción hormonal. La disfunción en este proceso contribuye a enfermedades metabólicas como la obesidad y la diabetes tipo II. Se han desarrollado modelos in vitro para investigar los mecanismos de la adipogénesis, y las células troncales de ligamento periodontal (CTLP) emergen como un modelo prometedor debido a su capacidad multipotente. Estudios previos han demostrado que la manipulación epigenética puede mejorar la respuesta adipogénica en varias líneas celulares. La acetilación de la lisina 9 en la histona H3 (H3K9ac) se asocia con la activación de genes clave, como PPARγ-2. En este estudio, evaluamos si los inhibidores de la histona desacetilasa de clase I, como el ácido valproico (VPA) y el butirato de sodio (NaBu), ambos ácidos grasos de cadena corta, pueden aumentar la acetilación de H3K9 e influir en la diferenciación adipogénica. Utilizamos concentraciones de VPA de 1, 4 y 8 mM y NaBu de 1, 2 y 5 mM para evaluar sus efectos sobre la viabilidad celular, la morfología, la distribución de H3K9ac y la diferenciación adipogénica. Los resultados indicaron que las células tratadas con NaBu de 5 mM presentaron cambios morfológicos, menor viabilidad, mayor intensidad de la señal de H3K9ac y mayor deposición lipídica intracelular. Estos resultados sugieren que la inhibición de las HDAC por NaBu aumenta la plasticidad hacia la adipogénesis de las CTLP mediante un cambio transcripcional limitado en sus genes clave.

PALABRAS CLAVE: Células troncales de ligamento periodontal; Acetilación de histonas; Adipogénesis; Inhibidores de histonas desacetilasas.

INTRODUCTION

Adipose tissue stores energy in the form of fat and possesses remarkable plasticity, enabling it to increase in size through hypertrophy (cell enlargement) and/or hyperplasia (increase in cell number) while retaining the ability to return to its basal state. It functions as an endocrine organ, regulating metabolic and hormonal processes. However, overnutrition can induce hypertrophy and disrupt adipogenesis, contributing to metabolic disorders such as obesity, type II diabetes, and metabolic syndrome (1). To better understand these pathologies, *in vitro* models have been developed to investigate the cellular and molecular mechanisms that regulate adipogenesis. Mesenchymal stem cells (MSCs), found in various tissues throughout the body, have been among the most widely used research models over the years. These cells possess self-renewal capability, exhibit a high proliferation rate, and can differentiate *in vitro* into various cell types when exposed to appropriate stimuli (2). A notable example is human periodontal ligament stem cells (PDLSCs), derived from fibrous connective tissue rich in collagen, proteins, and polysaccharides (3). PDLSCs represent a promising model for studying tissue regeneration, owing to their unique capacity for both adipogenic and osteogenic differentiation (4-6). Adipogenesis has primarily been investigated in murine MSC lines such as 3T3-L1. In these models, the process is divided into two stages: commitment and differentiation (7,8). Furthermore, epigenetic modifications play a significant role in regulating adipogenesis by influencing gene expression patterns and cellular differentiation processes (9). Specifically, these modifications are crucial for controlling chromatin dynamics and modulating the accessibility of transcriptional machinery to key regulatory regions (10). This facilitates the expression

of early genes, such as C/EBPβ, which promotes the expression of PPARγ, the master regulator of adipogenesis, thus facilitating the differentiation of preadipocytes into mature adipocytes (10,11). PPARγ has several isoforms, with PPARγ2 being predominantly found in adipose tissue, and its expression has been shown to be essential for this process (12). Additionally, it is important to evaluate the presence of late-stage genes in this process, such as ADIPOQ, whose protein product is adiponectin. This hormone promotes cell proliferation and preadipocyte differentiation (13).

Histone acetylation induces the relaxation of DNA coiling, facilitating transcription, while the removal of acetyl groups suppresses gene expression (14). A well-known epigenetic mark associated with transcriptional activation is the acetylation of lysine 9 on histone H3 (H3K9ac). Increased H3K9 acetylation has been documented during adipogenic differentiation in 3T3-L1 murine fibroblasts, where a positive correlation has been observed between acetylation levels and the activation of specific genes involved in the process (15). Two types of enzymes regulate histone acetylation: histone acetyltransferases (HATs), which add acetyl groups to histones, and histone deacetylases (HDACs), which remove these groups (16). This epigenetic modification plays a critical role in the adipogenic potential of various cell lines by modulating the ability of MSCs to differentiate into adipocytes. Acetylation is particularly linked to the expression of the PPARγ gene (17). By targeting the activity of HATs and HDACs, the adipogenic response of cells can be enhanced. Over the years, various studies have detected that the activity of HDAC1, HDAC2, HDAC3, and HDAC5 inhibits adipogenic differentiation in the 3T3-L1 cell line through the formation of protein complexes such as the mSin3A/HDAC1 complex (18-20). One approach to evaluate the role of class I histone deacetylases (HDACs) in adipogenesis is to inhibit their activity using histone deacetylase inhibitors (HDACis) and assess their impact on this process. HDACis are classified into four groups: hydroxamic acids, benzamides, cyclic peptides, and short-chain fatty acids, with the latter playing a modulatory role in MSCs differentiation (21). Valproic acid (VPA) and sodium butyrate (NaBu), which belong to the short-chain fatty acids group, exhibit selectivity for class I HDACs (22,23). The use of VPA and sodium butyrate has proven effective in enhancing the differentiation of MSCs, standing out for their low toxicity levels compared to other inhibitors such as TSA. VPA, primarily used in treating epilepsy, significantly impacts cell differentiation in various experimental models (24-27). Furthermore, it has been reported that VPA enhances lipid deposition in periodontal ligament MSCs, with a concomitant increase in H3K9 acetylation levels (28). Although global levels of H3K9ac provide indications of gene activation related to differentiation, immunocytochemical analysis could offer additional information on the distribution and localization of this epigenetic mark, providing a more detailed insight into its involvement in chromatin remodeling. On the other hand, NaBu, a product derived from bacterial fermentation in the large intestine, is considered one of the most potent inhibitors within the group of short-chain fatty acids. This compound has been used to promote the differentiation of bone marrow-derived MSCs into hepatocyte-like cells in three-dimensional cultures (29). It has also been shown to improve the adipogenic response in murine preadipocytes at a concentration of 0.5 mM (30). In this study, we investigated how histone deacetylase inhibitors (NaBu and VPA) modulate adipogenic differentiation in human PDLSCs, with a focus on the role of H3K9 acetylation in regulating their biological behavior. Understanding the epigenetic mechanisms in periodontal ligament stem cells may contribute to the development of dental strategies with HDAC inhibitors to direct cell differentiation during periodontal regeneration.

MATERIALS AND METHODS

CELLULAR CULTURE

In this study, cryopreserved PDLSCs from a 13-year-old male donor were used. The cells were obtained after the patient and his legal guardian provided signed informed consent in accordance with approval from the Research Ethics Committee of the Autonomous University of Yucatán (UADY) under approval number CIE-06-2017. The PDLSCs were cultured in an α-MEM-based medium (Minimum Essential Medium Eagle, Gibco) supplemented with 10% fetal bovine serum (FBS, Biowest) and 1% antibiotic-antimycotic solution (Gibco) in T25 culture flasks. The cultures were maintained in an incubator set at 37°C with 5% CO_2 until reaching passage number 6, at which point subsequent experimental assays were conducted.

EFFECT OF SODIUM BUTYRATE AND VALPROIC ACID ON THE MORPHOLOGY OF PDLSCS

To assess the effects of VPA and NaBu on the PDLSCs morphological, cells at passage 6 were seeded in a 12-well plate at a density of 5.6×10^3 cells/well. Cell counting was performed using a Neubauer chamber. After reaching 80% confluence, PDLSCs were pretreated for 72 hours with the HDAC inhibitors: 1, 4, and 8 mM VPA and 1, 2, and 5 mM NaBu. At the end of the treatment, the medium was removed, and the cells were washed with phosphate-buffered saline (PBS 1X, pH 7.4). Subsequently, 0.5% (w/v) crystal violet (HYCEL) was applied for 30 minutes, after which excess dye was removed. Following staining, the plates were examined under a Leica DM IL inverted contrast microscope (Leica Microsystems, Germany). A scale bar was added to the images using ImageJ software, with a Neubauer chamber as a reference.

DETERMINATION OF CELL VIABILITY ASSAY BY MTT

To analyze the effect of different concentrations of NaBu and VPA on the viability of PDLSCs, an MTT assay was performed using the MTT Cell Proliferation Assay Kit by Abcam (ab211091, USA). Cells were seeded in 96-well plates at a density of 10×10^3 cells per well and, after 24 hours, treated with 1, 2, and 5 mM NaBu and 1, 4, and 8 mM VPA for 72 hours. After the treatment, the culture medium was removed, and 100 µL of a 5% MTT solution was added to each well. The plates were incubated for three hours at 37 °C in a 5% CO_2 atmosphere. Finally, the medium was removed, 100 µL of MTT solvent was added to each well, and the absorbance was measured at 492 nm using an AMR-100 microplate reader (Hangzhou Allsheng Instruments Co., Ltd., China).

ADIPOGENIC INDUCTION

To assess the effects of different concentrations of VPA and NaBu on the adipogenesis of PDLSCs, cells were seeded at a density of 7×10^3 cells per well in 12 well plates. These cells were pretreated with the specified inhibitor concentrations for 72 hours. After pretreatment, the basal medium was replaced with an adipogenic induction medium consisting of α-MEM, 10% (v/v) SFB, penicillin (100 IU/mL), streptomycin (100 µg/mL), dexamethasone (1 µM), indomethacin (60 µM), 3-isobutyl-1-methylxanthine (IBMX, 500 µM), and human insulin (1.7 µM). Over 14 days, the medium was changed twice a week, and photographic monitoring was conducted using an inverted microscope.

IMMUNOCYTOCHEMICAL ANALYSIS OF H3K9AC

An immunocytochemical assay was performed to evaluate the effect of VPA and NaBu on

H3K9 acetylation in PDLSCs during adipogenesis. PDLSCs were seeded in Falcon® culture chambers at a density of 3 × 103 cells per well, with 100 µL of basal medium. Once 80% confluence was reached, the cells were treated with 8 mM VPA and 5 mM NaBu for 72 hours. The medium containing the inhibitor was then replaced with adipogenic medium, which was maintained for 21 days, with two medium changes per week. Cells were fixed with 4% formaldehyde and permeabilized using 0.2% Triton X-100. Blocking was performed with 2% bovine serum albumin, followed by overnight incubation at 4°C with a polyclonal antibody against H3K9ac (1:100 dilution) and H3(1:200 dilution) (Merck-Millipore, Darmstadt, Germany). The cells were then incubated for one hour at room temperature with the secondary antibody Goat Anti-Rabbit IgG H&L (Alexa Fluor® 488 (1:5000 dilution). Finally, they were counterstained with 4,6-diamidino-2-phenylindole (DAPI). Observations were made using a confocal microscope in collaboration with the UNAM Research Support Network (RAI). For each treatment, 12 photomicrographs were obtained from three different sections of four wells per inhibitor concentration. The mean fluorescence intensity of the photomicrographs was analyzed using the ROI (Region of Interest) tool in ImageJ software.

QUANTITATIVE PCR EVALUATION OF ADIPOGENIC MARKERS

To investigate how short-chain fatty acid inhibitors regulate the transcriptional expression of genes associated with adipogenic differentiation, cells were seeded in 12-well plates at a density of 15,000 cells/mL per well. Once the cells adhered, they were treated with inhibitors (5 mM NaBu and 8 mM VPA) for 72 hours. Untreated cells served as controls. Following pretreatment, the growth medium was replaced with an adipogenic induction medium. Total RNA was extracted on days 0, 14, and 21 after adipogenic induction using the TRIzol method. Complementary DNA (cDNA) synthesis was carried out using the RevertAid First-Strand cDNA Synthesis Kit (Thermo Scientific) according to the supplier's protocol. Gene expression was assessed by quantitative PCR (qPCR) using the iTaq™ Universal SYBR Green Supermix kit (Bio-Rad) in accordance with the manufacturer's instructions. The amplification protocol consisted of an initial denaturation at 95°C for 5 minutes, followed by 40 cycles of denaturation at 95°C for 15 seconds, primer-specific annealing for 30 seconds (temperatures detailed in Table 1) and extension at 72°C for 15 seconds. Gene expression was determined using the ΔΔCt method described by Livak and Schmittgen (2001), with β-actin serving as the internal control for normalization.

STATISTICAL ANALYSIS

Quantitative data obtained from the experiments will be presented as $\bar{X} \pm S$. Comparisons of cell viability, fluorescence intensity, and gene expression results will be conducted using a one-way analysis of variance (ANOVA), followed by Tukey's post hoc test to assess the significance of differences between treatments, with a significance level of $P<0.05$. Region of Interest (ROI) analysis was performed using ImageJ software to quantify mean fluorescence intensities for the statistical analysis of fluorescence intensity in photomicrographs. Since the data did not meet the assumptions of normality or homogeneity of variance, a nonparametric analysis of variance (Kruskal-Wallis test) was applied to assess differences in distribution between groups (treatments), followed by an appropriate post hoc test. The level of significance was $P<0.05$. All statistical analyses were carried out using GraphPad Prism software.

RESULTS

EFFECT OF SHORT-CHAIN FATTY ACIDS EPIGENETIC INHIBITORS ON MORPHOLOGY AND CELL VIABILITY OF PERIODONTAL LIGAMENT STEM CELLS

To analyze how VPA and NaBu affect the cellular characteristics of PDLSCs, crystal violet staining was used to assess morphology, and MTT assays were conducted to determine cell viability. PDLSCs exhibit a characteristic morphology (Figure 1.A images a and e), characterized by oval nuclei, bipolar shape, and long cytoplasmic extensions known as filopodia. Regarding the effect of the inhibitors on the morphology of the PDLSCs, the observed changes were dose-dependent; at higher concentrations of the inhibitor, the cells lost their characteristic fibroblastoid morphology. PDLSCs treated with 8 mM VPA displayed elongated filopodia, while those exposed to (5 mM) NaBu exhibited shorter, branched filopodia (Figure 1.A image d and h). These changes suggest a reorganization and alterations in cell adhesion dynamics induced by the epigenetic inhibitors. Regarding cell viability, 1 and 4 mM VPA concentrations resulted in increased viability, while a significant reduction was observed at 8 mM (20.593±5.22), indicating cytotoxicity at higher VPA concentrations (Figure 1.B). In contrast, NaBu concentrations did not cause significant differences in cell viability compared to the control group (Figure 1.C).

EFFECT OF SHORT-CHAIN FATTY ACIDS EPIGENETIC INHIBITORS ON THE ADIPOGENIC DIFFERENTIATION OF PDLSCS

Photographic monitoring was conducted to study the effect of 1 and 8 mM VPA and 2 and 5 mM NaBu concentrations on the adipogenesis of PDLSCs. The impact of different concentrations of VPA (1, 4, 8 mM) and NaBu (1, 2, 5 mM) on cell morphology and viability was previously evaluated. The concentrations of 8 mM VPA and 5 mM NaBu were selected because they altered cell morphology. In the cell viability assay, a significant decrease in this parameter was observed in cells treated with 8 mM VPA. Additionally, lower concentrations (1 mM VPA and 2 mM NaBu) were included to assess whether there were differences in the adipogenic response based on the concentration of the inhibitor. On day 7 post-induction, lipid vacuoles were observed in the control group, and PDLSCs were exposed to the highest concentrations of 8 mM VPA and 5 mM NaBu. However, the characteristics of these vacuoles differed between groups: the control group exhibited a single large lipid vacuole surrounded by smaller vacuoles (Figure 2.A image b and k), whereas the inhibitor treated PDLSCs displayed the formation of two or more large lipid vacuoles, along with smaller ones (Figure 2.A image h and p). These findings suggest variations in lipid accumulation across groups. By day 14 post-induction, lipid vacuoles were present at all concentrations. A similar pattern was observed in the control, 1 mM VPA, and 2 mM NaBu groups, where a single large lipid vacuole or none, surrounded by smaller vacuoles, predominated (Figure 2.A-Figure 2.B image c, f, l, and ñ). In contrast, the 8 mM VPA and 5 mM NaBu groups exhibited a higher number of large lipid vacuoles (Figure 2.A-Figure 2.B image i and q).

EFFECT OF SHORT-CHAIN FATTY ACIDS EPIGENETIC INHIBITORS ON H3K9 ACETYLATION IN PDLSCS

In the study by Serralta-Interian *et al*. (28), an increase in global levels of H3K9ac was reported in PDLSCs induced to undergo adipogenesis at day 21 following the use of histone deacetylase inhibitors. Based on their findings, an immunocytochemical assay was performed on day 21 of this study to assess the distribution patterns of H3K9ac in these cells during adipogenic differentiation. An immunocytochemical assay was performed on day 21, using concentrations of 8 mM of VPA and 5 mM of NaBu. Lower concentrations (1 mM of VPA and 2 mM of NaBu) induced the formation of small lipid vacuoles up to day 14. In comparison,

higher concentrations promoted the formation of larger vacuoles, indicating a more advanced stage of adipogenic differentiation. The detection of the anti-H3K9ac antibody showed positive results across all groups. Control cells exhibited a diffuse distribution of H3K9ac foci being observed in the control cells (Figure 3.A image a). In contrast, cells treated with inhibitors displayed a perinuclear distribution of H3K9ac foci co-localizing with DAPI staining (Figure 3.A images f and i). Furthermore, the fluorescence intensity of H3K9ac was significantly higher in VPA and NaBu-treated cells (Figure 3.A images d and g). Quantitative analysis (Figure 3.B) showed an increase in the percentage of cells surpassing the average fluorescence intensity of control cells. VPA-treated cells reached 92.6% of cells with intensity above the average value, while NaBu-treated cells showed 74% (Figure 3.B). Differences are statistically significant, as determined by Kruskal-Wallis analysis. In the immunocytochemical assay, nuclear colocalization was observed, coinciding with the distribution of H3K9ac (Figure 3.C). In qualitative analysis (Figure 3.D), cells treated with inhibitors showed increased fluorescence, where approximately 75% of the control cells had a lower mean average fluorescence intensity than the inhibitor-treated cells.

EFFECT OF SHORT-CHAIN FATTY ACIDS EPIGENETIC INHIBITORS ON GENE EXPRESSION OF MARKERS ASSOCIATED WITH ADIPOGENESIS IN PDLSCS

Key marker genes were analyzed to investigate the involvement of CEBP, PPARγ2, and ADIPOQ gene expression in the differentiation of PDLSCs into adipocytes. The relative expression of the CEBPβ gene varied depending on the group evaluated and the stages of the adipogenic process. In the control group, a progressive decrease was observed from day 0, with the highest value at the beginning and the lowest at day 21, reflecting a natural reduction without intervention. In cells treated with VPA, a marked suppression was observed between days 0 and 14, followed by a slight recovery in the later stages, suggesting that this inhibitor primarily impacts the early phases of CEBPβ expression. In contrast, in cells treated with NaBu, a mild activation was observed between days 0 and 14, followed by a drastic decrease at day 21, indicating a potentiating effect in the intermediate stages but significant inhibition in the later phases of the adipogenic process (Figure 4.A).

The relative expression of the PPARγ2 gene varied depending on the treatment and stages of the process. In the control group, a marked increase was observed between days 0 and 14, reaching its peak at this point, followed by a decrease at day 21. This suggests activation during the intermediate stage, followed by a decline in later stages. In cells treated with VPA, expression increased slightly at first, with values remaining stable between days 14 and 21, indicating a moderate effect of this inhibitor on expression during this stage. In cells treated with NaBu, a strong increase in expression was observed between days 0 and 14, followed by a significant reduction at day 21, reflecting activation during the intermediate stage followed by inhibition in the later stages (Figure 4.B).

The relative expression of the ADIPOQ gene showed distinct patterns depending on the evaluated group. In the control group, expression increased and peaked on day 14, followed by a slight decrease on day 21, suggesting an initial activation that later diminished. In VPA-treated cells, expression also peaked on day 14 but decreased significantly on day 21, indicating marked activation in the intermediate stages followed by inhibition in later stages. In NaBu-treated cells, the pattern was similar, with a sharp increase on day 14 followed by a drastic decrease on day 21, reflecting activation in the intermediate stages and inhibition in the later phases of adipogenic differentiation (Figure 4.C).

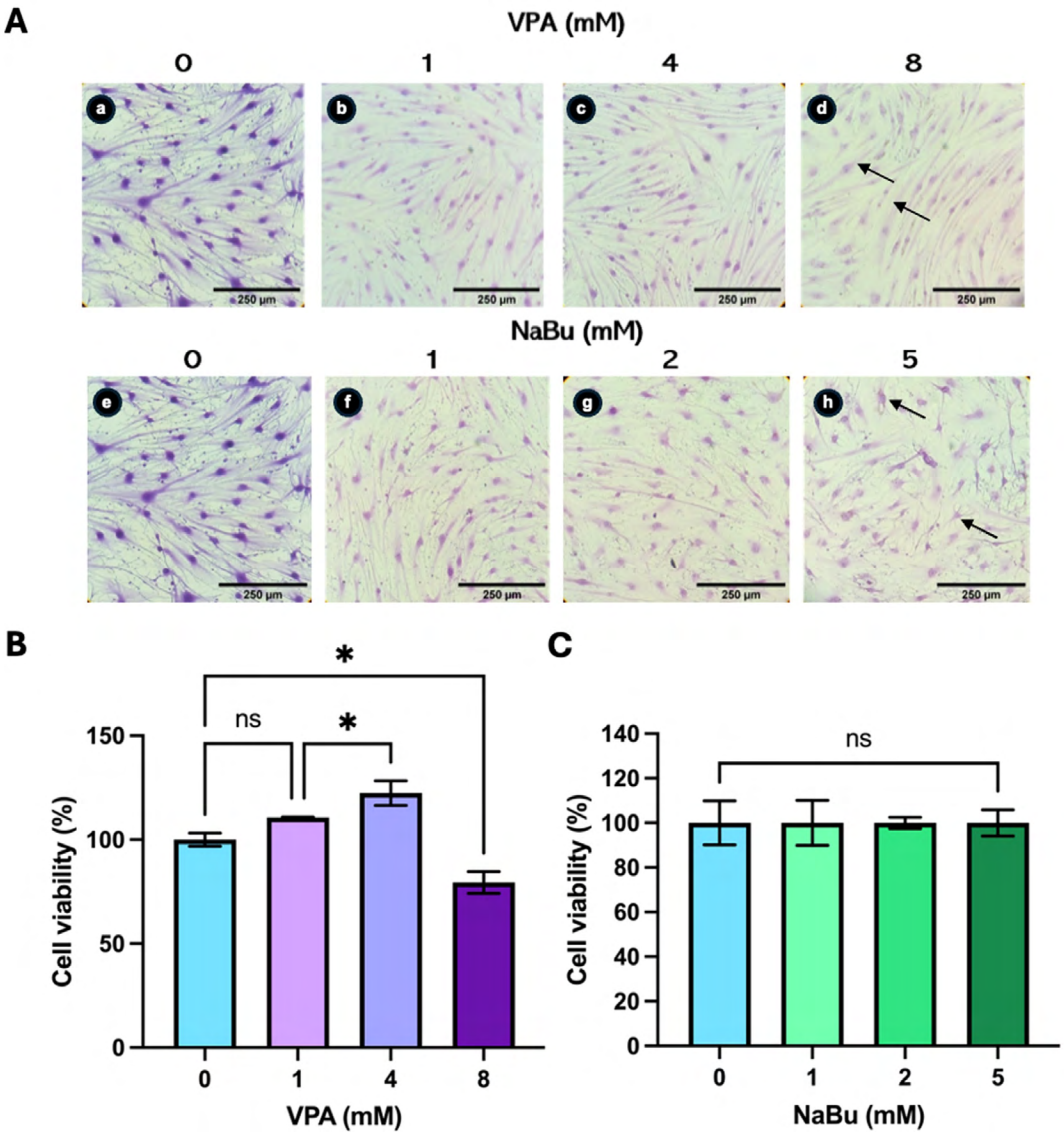

Figure 1. Cell viability and morphology of PDLSCs at different concentrations of VPA and NaBu. (A) Morphology of PDLSCs exposed to 1, 4, and 8 mM VPA, and 1, 2, and 5 mM NaBu after 72 h of treatment. Objective at 20x. (B) Cell viability of PDLSCs exposed to 1, 4, and 8 mM VPA after 72 h of treatment. (C) Cell viability of PDLSCs exposed to 1, 2 mM, and 5 mM NaBu after 72 h of treatment. Values represent mean±standard error of n=3. Significant differences between data sets are indicated by asterisks above error bars ($P<0.05$).

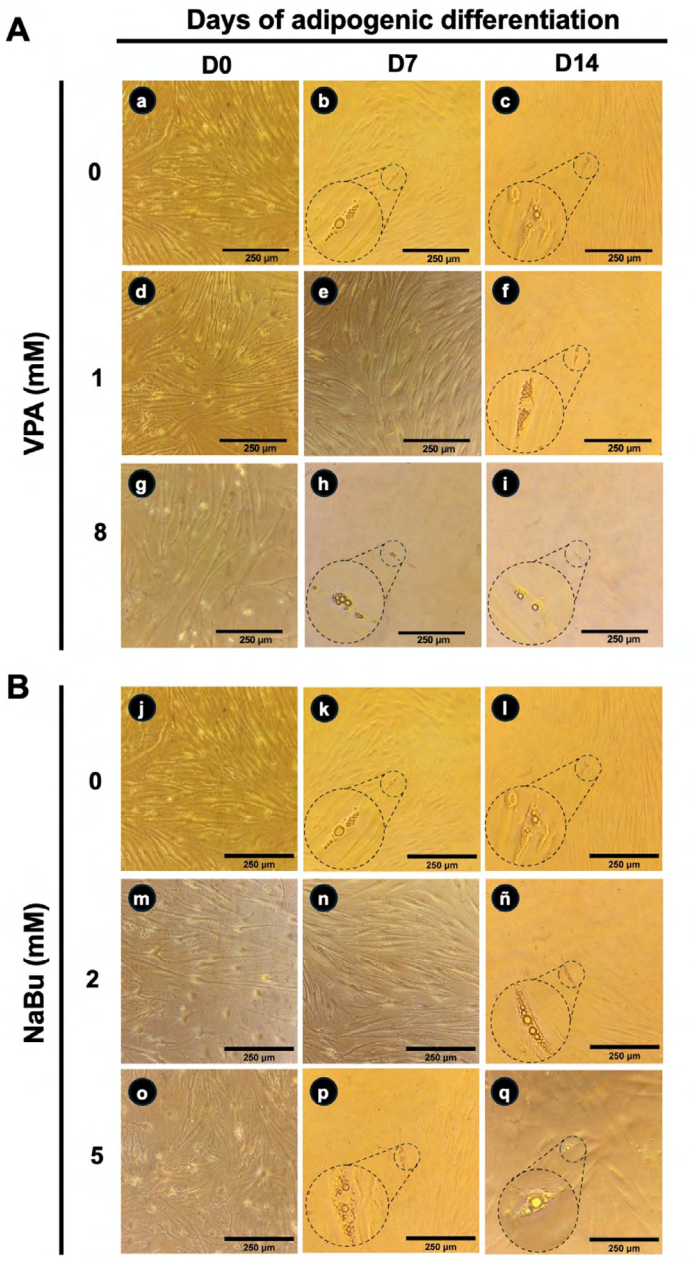

Figure 2. Morphological assessment of the response to adipogenic induction of PDLSCs exposed to NaBu and VPA. (A) PDLSCs corresponding to the control (a, b, and c) and PDLSCS exposed to a concentration of 1 mM and 8 mM VPA (d, e, f, g, h and i). (B) PDLSCs corresponding to the control (j, k, and l) and PDLSCs exposed to a concentration of 2 mM and 5 mM NaBu (m, n, ñ, o, p and q). Cells were incubated with the defined adipogenic induction medium. Circles indicate cells with lipid vacuoles. Photomicrographs were obtained with a 20X objective. The scale-bar corresponds to 250 µm.

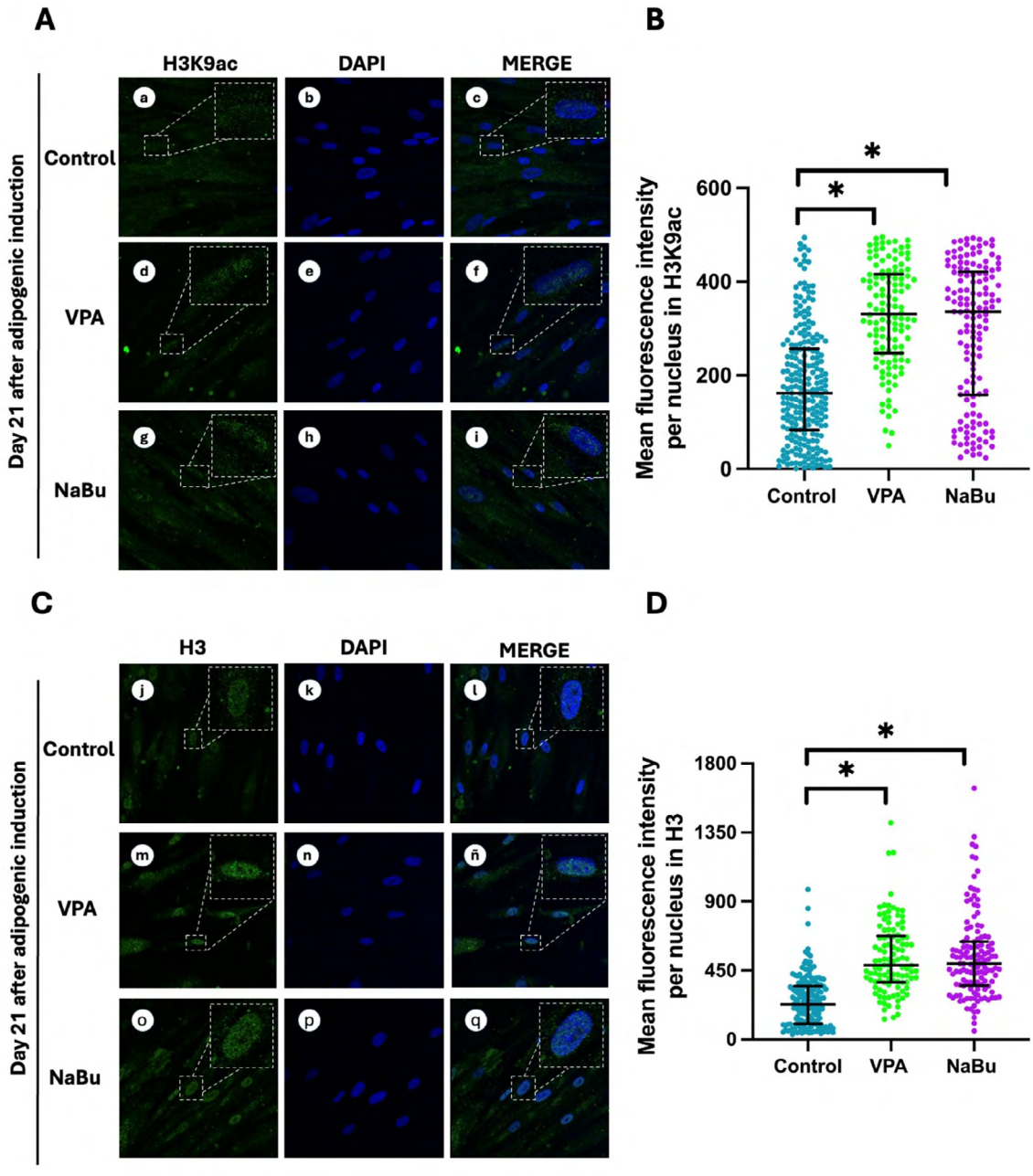

Figure 3. Analysis of the distribution of H3K9ac and H3 mean fluorescence intensity in cells with and without treatment with short-chain fatty acid inhibitors on day 21 post adipogenic induction. (A) Photomicrographs of the H3K9 fluorescence signal in PDLSCs treated with 8 mM VPA and 5 mM NaBu and without inhibitors (Control). (B) Analysis of the distribution of the mean intensity of H3K9ac fluorescence in the three PDLSCS treatments using the Kruskal-Wallis test. The duration of treatment with inhibitors was 72 hours. (C) Photomicrographs of the H3 fluorescence signal in PDLSCs treated with 8 mM VPA and 5 mM NaBu, and Control. (D) Analysis of the distribution of the mean intensity of H3 fluorescence in the three PDLSCS treatments using the Kruskal-Wallis test. Values represent the median ± interquartile range (n=12). Asterisks on the graph indicate significant differences between groups according to the Kruskal-Wallis test ($p<0.05$).

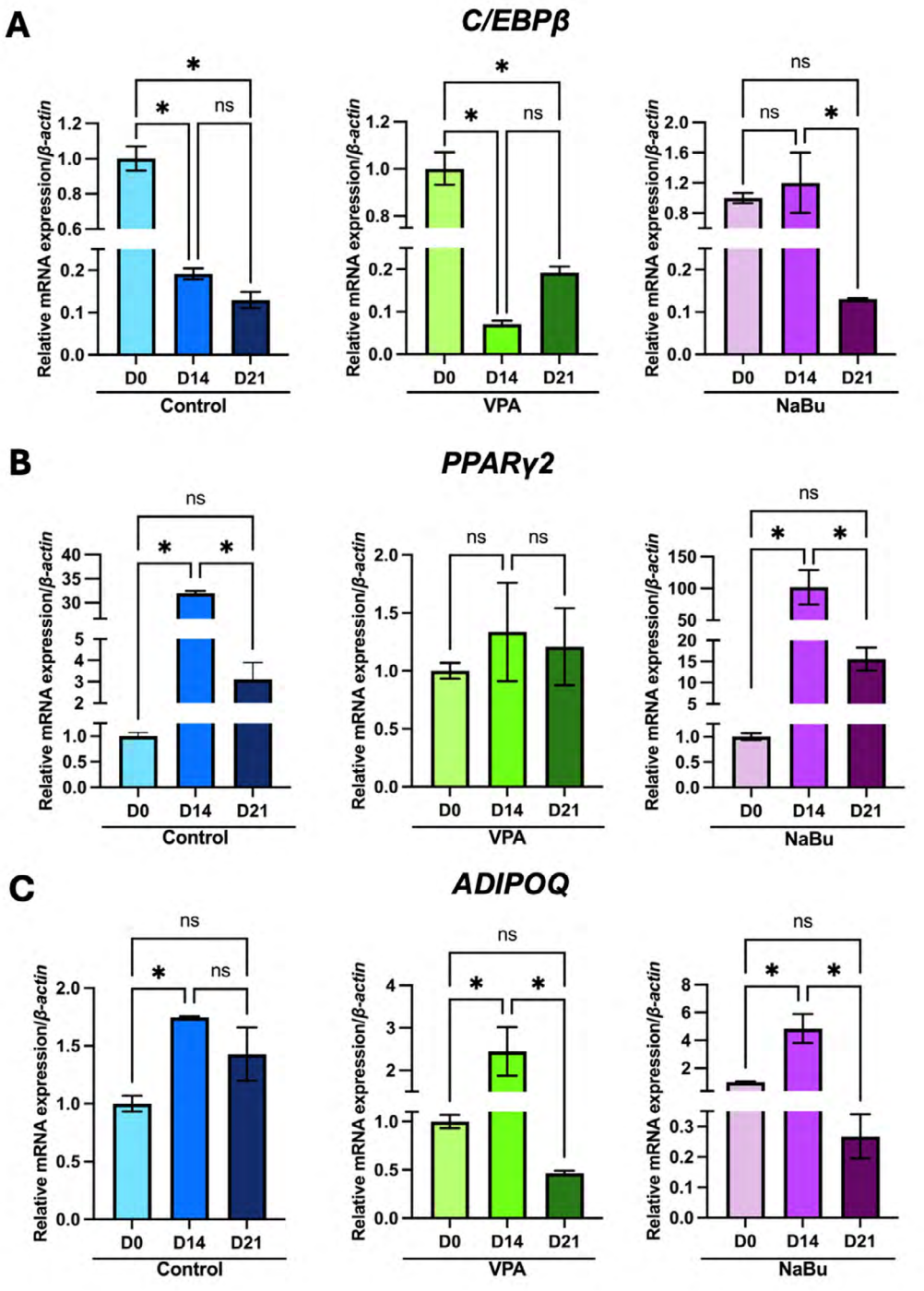

Figure 4. Relative expression of C/EBPβ (A), PPARγ2 (B), and ADIPOQ (C) in PDLSCs without histone deacetylase inhibitors, pretreated with 8 mM VPA, and 5 mM NaBu for 72 hours. The data represent normalized relative mRNA expression levels using β-Actin as the housekeeping gene. Transcript levels are presented as mean±standard deviation (n=2). Statistical significance was evaluated by ANOVA with Tukey's pos hoc, and significant differences between data sets are indicated by asterisks above error bars ($P<0.05$).

DISCUSSION

VPA and NaBu are short-chain fatty acids that have been used in various in vitro models due to their ability to modulate cell differentiation as inhibitors of HDACs (25-27). The morphology of PDLSCs showed a dose-dependent response to these inhibitors. PDLSCs typically exhibit a fibroblastoid-like morphology with oval nuclei and long cytoplasmic extensions known as filopodia. However, 8 mM of VPA caused the filopodia to elongate, while 5 mM of NaBu caused the filopodia to shorten, resulting in a branched cell appearance.

These observations are consistent with those reported by Lee *et al*. (31), where human gingival-derived mesenchymal stem cells (hGMSCs) exposed to high concentrations of VPA (8 mM) lost their characteristic fibroblastoid shape and adopted a more flattened morphology. VPA-induced morphological changes in hGMSCs and PDLSCs (evidenced by the elongation of filopodia). One possible explanation is that VPA modulates the PDLSCs, which are thought to be mediated by their effects on the cytoskeleton, including alterations in actin organization and focal adhesion-associated signaling pathways. For example, in L929 murine fibroblasts, 1 mM VPA increased F-actin polymerization and elevated expression of key proteins such as focal adhesion kinase (FAK), paxillin, and vinculin. Conversely, in renal cancer cells, VPA treatment at the same concentration reduced FAK activation and upregulated the expression of integrin subtypes α3, α5, and β3, influencing cell motility and structural organization (32).

On the other hand, NaBu has been shown to alter the organization of actin filaments in murine brain endothelial cells when used at a concentration of 1 μm (33). Additionally, NaBu can inhibit the activity of the nuclear transcription factor NF-κB, reducing its gene transcription activity. Although the impact of NF-κB on the regulation of tight junction proteins has not been fully elucidated, it has been proposed that NaBu, through its inhibition of histone deacetylases (HDACs), may induce hyperacetylation of the p65 subunit of NF-κB. This post-translational modification could disrupt the interaction of p65 and its inhibitor IκB, negatively modulating NF-κB transcriptional activity. This suggests a potential mechanism for the regulation of tight junctions mediated by this factor (34).

Another important parameter in the culture of stem cells is their viability, as it indicates that the cells are in a healthy and functional state. A viable cell can respond to signals promoting specialization towards a specific lineage. The results revealed that the concentration of 8 mM of VPA reduced cell viability to 80%, which, according to the ISO 10993-5 standard, is classified as slightly cytotoxic. This standard considers viability percentages between 80% and 60% indicative of slight cytotoxicity (35). The observed reduction in cell viability at higher VPA concentrations aligns with findings reported by Yu *et al*. (36), who documented a dose-dependent decrease in the proliferation of tonsil-derived mesenchymal stem cells exposed to 1-5 mM VPA for 72 hours. An interesting observation was reported by Lee *et al*.(31), who indicated that although 8 mM VPA reduced the viability of hGMSCs, these cells retained their ability to differentiate into osteocytes. This was evidenced by the formation of calcium deposits, albeit in smaller amounts compared to cells without VPA treatment. The ability of hGMSCs to retain their potential to differentiate into osteocytes may be attributed to the absence of apoptosis in these cells.

PDLSCs exposed to an 8 mM concentration of VPA may have entered a state of proliferation inhibition or cytostatic effect, as it has been documented that in cancer cell lines such as MCF-7, VPA induces cell growth inhibition by stopping the cell cycle in the G1 phase (37).

The cell cycle is primarily regulated during the differentiation phase of adipogenesis. For

instance, in murine fibroblast cell cultures, the confluence of preadipocytes causes contact inhibition, leading to cell cycle arrest. Subsequently, synthetic stimulation with dexamethasone, insulin, and/or intracellular cAMP enhancers induces the generation of preadipocytes through mitotic clonal expansion, a critical step in the terminal differentiation of adipocytes (38). This suggests that VPA, by inducing a cytostatic effect in various cell lines, might accelerate adipogenesis by promoting cell cycle arrest.

The effect of short-chain fatty acid inhibitors, such as VPA and NaBu, on PDLSCs favored the formation of larger lipid vacuoles compared to those observed in the control. This could be due to the inhibitors stimulating the formation of expanding lipid vacuoles (ELVs). ELVs contain a key enzyme for triglyceride biosynthesis, called glycerol-3-phosphate acyltransferase 4 (GPAT4), allowing rapid expansion of ELVs under fatty acid excess. This contrasts with static lipid vacuoles (SLVs), which are smaller because they do not have access to the endoplasmic reticulum or the enzymes necessary for triglyceride synthesis (39). The localization and morphology of SLVs and ELVs observed in this study align with those previously described in the literature. For example, in the photomicrographs of the control group on day 7 (Figure 2.A image b), the SLVs are found at the ends of the cells, and there is an ELV in the center of the cell. However, in the concentrations of 5 mM NaBu and 8 mM VPA (Figure 2 images h and p), a greater number of ELVs were found predominantly clustered in the center of the cell. The influence of NaBu and VPA on the formation and distribution of ELVs suggests an improvement in the adipogenic response, as they promote lipid accumulation and may facilitate a more efficient differentiation towards mature adipocytes.

Recently, various studies have found that using inhibitors of the short-chain fatty acid type can increase the adipogenic potential of cells. For example, Tugnoli *et al*. (40) observed that the presence of NaBu could induce adipogenesis in porcine tissue-derived mesenchymal stem cells in a basal medium. They found that increasing concentrations of NaBu were associated with an increase in the formation of lipid vacuoles, which correlated with an increase in the gene expression of key genes in adipogenesis, including C/EBPα, PPARγ, LPL, and FABP4. Specifically, on day 3, after exposure to a basal medium with a 5 mM NaBu concentration, the maximum peak expression of these four genes was reached. Over a period of 27 days, the transcripts of these genes decreased, highlighting the temporal regulation of adipogenic genes at key moments of adipogenesis. This experiment showed that NaBu enhanced the expression of C/EBPα, PPARγ, LPL, and FABP4 at a specific stage of the adipogenic process, which increased the adipogenic capacity of cells.

Likewise, Serralta-Interian *et al*. (28) reported that PDLSCs exposed to 8 mM of VPA increased lipid deposition compared to the control, which was also associated with a threefold increase in the expression of ADIPOQ compared to the control at day 21 of adipogenic induction. However, the expression analysis of PPARγ exhibited no significant increase in this gene at the same time point. This could be related to the fact that PPARγ is a gene whose expression predominates in the intermediate stages of adipogenesis. As the process progresses, it could be downregulated, coinciding with the activation of characteristics of late phases, such as ADIPOQ. This study showed that the expression of adipogenic markers varies depending on the stage of the adipogenic process.

The expression of adipogenic markers at specific times allows modulation of the adipogenic response of stem cells. It has been shown that the increase in the early expression of PPARγ2 can improve the adipogenic capacity of cells (40). The results obtained in the temporal analysis of the expression of C/EBPβ, PPARγ, and ADIPOQ in this

experiment coincide with the expected pattern of the normal adipogenic process. In this context, day 14 marks the peak expression of genes such as C/EBPβ and PPARγ, associated with the early and intermediate phases of adipogenesis.

Regarding inhibitors, cells treated with 5 mM NaBu showed a three-fold increase in PPARγ2 expression at day 14 compared to the control group. Conversely, those treated with 8 mM of VPA did not show significant increases in the expression of the evaluated transcripts. This could be related to the fact that, within the group of short-chain fatty acids, sodium butyrate presents a greater selectivity for class I HDACs, such as HDAC3, with an IC50 value of 0.318 mM (22).

When evaluating the effect of epigenetic inhibitors on the spatial distribution of H3K9ac in PDLSCs during adipogenic induction using immunocytochemistry, a perinuclear distribution of H3K9ac was observed. Statistical analysis using the Kruskal-Wallis test revealed a significant increase in the percentage of cells with a higher intensity of H3K9ac fluorescence in cells treated with VPA or NaBu compared to the control group. Similarly, in the study by Stachecka *et al.*(41), it was reported that the spatial distribution and levels of euchromatin histone marks, such as H4K8ac and H3K9ac, were altered in porcine mesenchymal stem cells (AD-MSCs) during adipogenesis. Specifically, H3K9ac was detected at the periphery of adipocyte nuclei, which aligns with our findings. However, the study of the effects of these inhibitors on the distribution of H3K9ac during adipogenesis remains poorly documented, highlighting the need for further research to better understand these mechanisms.

Serralta-Interian *et al*. (28) reported that PDLSCs isolated from the periodontal ligament of a 15-year-old male donor and treated with histone deacetylase inhibitors, such as VPA and trichostatin A (TSA), showed reductions of 70% and 30% in H3K9 acetylation levels, respectively, after 72 hours of treatment compared to the control. During adipogenic induction, these values were modified, with a 30% increase in acetylation observed with TSA treatment, whereas VPA resulted in a 70% decrease in H3K9ac compared to the control group.

The effect of VPA on H3K9 acetylation during adipogenesis has also been evaluated by Montero-Del-Toro *et al*. (42) who analyzed the levels of this protein on days 0 and 28 of adipogenic induction. Their study highlighted that using the adipogenic medium without inhibitors, the levels of H3K9ac were elevated at the early stage (day 0) compared to cells pretreated with inhibitors. This was associated with chromatin remodeling induced by the components of the medium. However, over time, inhibitor-treated cells exhibited increased levels of H3K9ac by day 28 of adipogenic induction. Furthermore, this study also observed that using inhibitors such as VPA in PDLSCs could favor the formation of lipid vacuoles, which was reflected in an increase in lipid deposition.

The findings suggest that short-chain fatty acid epigenetic inhibitors modulate the distribution and levels of H3K9ac in a cell state-dependent manner. This modification could promote chromatin opening, facilitating the access of transcriptional machinery, such as RNA polymerase, to genes involved in cell differentiation. Specifically, the activation of PPARγ2, a key regulator of adipogenesis, may enhance the differentiation of mesenchymal stem cells into adipocytes. Notably, NaBu significantly increased PPARγ2 expression at day 14 and induced the formation of larger lipid vacuoles, indicating a more advanced stage of adipogenic differentiation.

CONCLUSION

Short-chain fatty acids, such as VPA and NaBu, have been shown to enhance the adipoge-

nic response in PDLSCs, as evidenced by increased intracellular lipid deposition and the regulation of adipogenic markers (C/EBPα, PPARγ-2, and ADIPOQ). Among the inhibitors tested, NaBu stands out for increasing the expression of PPARγ-2 and exhibited a significant increase in the H3K9ac fluorescence signal, suggesting that this compound may enhance the presence of this specific epigenetic mark. However, further studies are needed to elucidate the mechanisms by which epigenetic inhibitors influence H3K9ac and to determine whether these perturbations directly trigger an enhanced adipogenic response or involve additional metabolic pathways. Our results demonstrate that sodium butyrate, through specific inhibition of class I HDACs, significantly promotes adipogenesis in periodontal ligament stem cells. These findings suggest that epigenetic modulation via selective HDAC inhibitors could emerge as a key strategy for controlling cell fate during periodontal regeneration, paving the way for the development of more targeted therapies.

CONFLICT OF INTEREST: The authors declare that they have no conflicts of interest.

AUTHOR CONTRIBUTION STATEMENT

Conceptualization: B.A.R.J.
Methodology and validation: A.T.N. and A.A.S.I.
Data analysis and interpretation: A.T.N., A.A.S.I., G.N.C. and B.A.R.J.
Writing-original draft preparation: A.T.N. and A.A.S.I.
Writing-review & editing: B.A.R.J., R.A.R.S. and L.C.C.

ACKNOWLEDGMENTS

This study was supported by Secretaria de Ciencia, Humanidades, Tecnología e Innovación (SECIHTI) grants awarded to Beatriz A. Rodas-Junco (Ciencia de Frontera-429849), postdoctoral fellowship for Angelica Serralta-Interian (No. 474112), and a fellowship for Anahí Torres-Najera (No.1323464). The authors acknowledge the support of the Laboratorio de Células Troncales de la Facultad de Odontología and Facultad de Ingeniería Química de la Universidad Autónoma de Yucatán and the Seeding Labs program.

REFERENCES

1. De Fano M., Malara M., Vermigli C., Murdolo G. Adipose Tissue: A Novel Target of the Incretin Axis? A Paradigm Shift in Obesity-Linked Insulin Resistance. Int J Mol Sci. 2024; 25 (16).
2. Rodríguez-Fuentes D.E., Fernández-Garza L.E., Samia-Meza J.A., Barrera-Barrera S.A., Caplan A.I., Barrera-Saldaña H.A. Mesenchymal Stem Cells Current Clinical Applications: A Systematic Review. Arch Med Res. 2021; 52 (1): 93-101.
3. Thant L., Kaku M., Kakihara Y., Mizukoshi M., Kitami M., Arai M., et al. Extracellular Matrix-Oriented Proteomic Analysis of Periodontal Ligament Under Mechanical Stress. Front Physiol. 2022; 13: 899699.
4. Iwayama T., Sakashita H., Takedachi M., Murakami S. Periodontal tissue stem cells

and mesenchymal stem cells in the periodontal ligament. Jpn Dent Sci Rev. 2022; 58: 172-8.
5. Trejo Iriarte C.G., Ramírez Ramírez O., Muñoz García A., Verdín Terán S.L., Gómez Clavel J.F. Aislamiento de células mesenquimales del ligamento periodontal de premolares extraídos. Método simplificado. Rev. Odont. Mex. 2017; 21 (1): 13-21.
6. Wu Y., Wang Y., Ji Y., Ou Y., Xia H., Zhang B., et al. C4orf7 modulates osteogenesis and adipogenesis of human periodontal ligament cells. Am J Transl Res. 2017; 9 (12): 5708.
7. Matsushita K., Dzau V.J. Mesenchymal stem cells in obesity: insights for translational applications. Lab. Invest. 2017; 97 (10): 1158-66.
8. Musri M.M., Gomis R., Párrizas M. A chromatin perspective of adipogenesis. Organogenesis. 2010; 6 (1): 15-23.
9. Argaez-Sosa A.A., Rodas-Junco B.A., Carrillo-Cocom L.M., Rojas-Herrera R.A., Coral-Sosa A., Aguilar-Ayala F.J., et al. Higher Expression of DNA (de)methylation-Related Genes Reduces Adipogenicity in Dental Pulp Stem Cells. Front Cell Dev Biol. 2022; 10: 791667.
10. Musri M.M., Gomis R., Párrizas M. Chromatin and chromatin-modifying proteins in adipogenesis. Biochem Cell Biol. 2007; 85 (4): 397-410.
11. Zhang Q., Ramlee M.K., Brunmeir R., Villanueva C.J., Halperin D., Xu F. Dynamic and distinct histone modifications modulate the expression of key adipogenesis regulatory genes. Cell Cycle. 2012; 11 (23): 4310-22.
12. Hu W., Jiang C., Kim M., Xiao Y., Richter H.J., Guan D., et al. Isoform-specific functions of PPARγ in gene regulation and metabolism. Genes Dev. 2022; 36 (5-6): 300-12.
13. Fu Y., Luo N., Klein R.L., Garvey W.T. Adiponectin promotes adipocyte differentiation, insulin sensitivity, and lipid accumulation. J Lipid Res. 2005; 46 (7): 1369-79.
14. Mortada I., Mortada R. Epigenetic changes in mesenchymal stem cells differentiation. Eur J Med Genet. 2018; 61 (2): 114-8.
15. Steger DJ, Grant GR, Schupp M, Tomaru T, Lefterova MI, Schug J, et al. Propagation of adipogenic signals through an epigenomic transition state. Genes Dev. 2010; 24 (10): 1035-44.
16. King J., Patel M., Chandrasekaran S. Metabolism, HDACs, and HDAC Inhibitors: A Systems Biology Perspective. Metabolites. 2021; 11 (1): 792.
17. Jang S., Hwang J., Jeong H-S. The Role of Histone Acetylation in Mesenchymal Stem Cell Differentiation. Chonnam Med J. 2022; 58 (1): 6-12.
18. Yoo E.J., Chung J.J., Choe S.S., Kim K.H., Kim J.B. Down-regulation of histone deacetylases stimulates adipocyte differentiation. J Biol Chem. 2006; 281 (10): 6608-15.
19. Kuzmochka C., Abdou H-S, Haché R.J.G., Atlas E. Inactivation of Histone Deacetylase 1 (HDAC1) But Not HDAC2 Is Required for the Glucocorticoid-Dependent CCAAT/Enhancer-Binding Protein α (C/EBPα) Expression and Preadipocyte Differentiation. Endocrinology. 2014; 155 (12): 4762-73.
20. Pant R., Alam A., Choksi A., Shah V.K., Firmal P., Chattopadhyay S. Chromatin remodeling protein SMAR1 regulates adipogenesis by modulating the expression of PPARγ. Biochim. Biophys. Acta Mol. Cell Biol. Lipids. 2021; 1866 (12): 159045.
21. Lagace D.C., Nachtigal M.W. Inhibition of histone deacetylase activity by valproic acid blocks adipogenesis. J Biol Chem. 2004; 279 (18): 18851-60.
22. Ho R.H., Chan J.C.Y., Fan H., Kioh D.Y.Q., Lee B.W., Chan E.C.Y. In Silico and in Vitro Interactions between Short Chain Fatty Acids and Human Histone Deacetylases. Biochemistry. 2017; 56 (36): 4871-8.
23. Sixto-López Y., Bello M., Correa-Basurto J. Exploring the inhibitory activity of valproic

acid against the HDAC family using an MMGBSA approach. J Comput Aided Mol Des. 2020; 34 (8): 857-78.
24. Romoli M., Mazzocchetti P., D'Alonzo R., Siliquini S., Rinaldi V.E., Verrotti A., et al. Valproic Acid and Epilepsy: From Molecular Mechanisms to Clinical Evidences. Curr Neuropharmacol. 2019; 17 (10): 926-46.
25. Fu Y., Zhang P., Ge J., Cheng J., Dong W., Yuan H., et al. Histone deacetylase 8 suppresses osteogenic differentiation of bone marrow stromal cells by inhibiting histone H3K9 acetylation and RUNX2 activity. Int J Biochem Cell Biol. 2014; 54: 68-77.
26. Santos J., Hubert T., Milthorpe B.K. Valproic Acid Promotes Early Neural Differentiation in Adult Mesenchymal Stem Cells Through Protein Signalling Pathways. Cells. 2020; 9 (3).
27. Um S., Lee H., Zhang Q., Kim H.Y., Lee J-H, Seo B.M. Valproic Acid Modulates the Multipotency in Periodontal Ligament Stem Cells via p53-Mediated Cell Cycle. Tissue Eng Regen Med. 2017; 14 (2):153-62.
28. Serralta-Interian A., Toro J., Nic Can G., Rojas Herrera R., Aguilar-Ayala F.J., Rodas-Junco B. Inhibition of histone deacetylases class I improves adipogenic differentiation of human periodontal ligament cells. Cell Mol Biol. 2024; 70: 40-7.
29. Rashid S., Salim A., Qazi R-E-M, Malick T.S., Haneef K. Sodium Butyrate Induces Hepatic Differentiation of Mesenchymal Stem Cells in 3D Collagen Scaffolds. Appl Biochem Biotechnol. 2022; 194 (8): 3721-32.
30. Eung J.Y., Chung J.J., Sung S.C., Kang H.K., Jae B.K. Down-regulation of histone deacetylases stimulates adipocyte differentiation. J Biol chem. 2006; 281 (10): 6608-15.
31. Lee H., Lee J.Y., Ha D-H, Jeong J-H, Park J-B. Effects of Valproic Acid on Morphology, Proliferation, and Differentiation of Mesenchymal Stem Cells Derived From Human Gingival Tissue. Implant Dent. 2018; 27 (1): 33-42.
32. Jones J., Juengel E., Mickuckyte A., Hudak L., Wedel S., Jonas D., et al. Valproic acid blocks adhesion of renal cell carcinoma cells to endothelium and extracellular matrix. J Cell Mol. 2009; 13 (8b): 2342.
33. Knox E.G., Aburto M.R., Tessier C., Nagpal J., Clarke G., O'Driscoll C.M., et al. Microbial-derived metabolites induce actin cytoskeletal rearrangement and protect blood-brain barrier function. iScience. 2022; 25 (12): 105648.
34. Fock E., Parnova R. Mechanisms of Blood-Brain Barrier Protection by Microbiota-Derived Short-Chain Fatty Acids. Cells. 2023; 12 (4).
35. López-García J., Lehocký M., Humpolíček P., Sáha P. HaCaT Keratinocytes Response on Antimicrobial Atelocollagen Substrates: Extent of Cytotoxicity, Cell Viability and Proliferation. J Funct Biomater. 2014; 5 (2): 43-57.
36. Yu Y., Oh S-Y, Kim H.Y., Choi J-Y, Jo S.A., Jo I. Valproic Acid-Induced CCN1 Promotes Osteogenic Differentiation by Increasing CCN1 Protein Stability through HDAC1 Inhibition in Tonsil-Derived Mesenchymal Stem Cells. Cells. 2022; 11 (3).
37. Ma X-J, Wang Y-S, Gu W-P, Zhao X. The role and possible molecular mechanism of valproic acid in the growth of MCF-7 breast cancer cells. Croat Med J. 2017; 58 (5): 349-57.
38. Dowker-Key P.D., Jadi P.K., Gill N.B., Hubbard K.N., Elshaarrawi A., Alfatlawy N.D., et al. A Closer Look into White Adipose Tissue Biology and the Molecular Regulation of Stem Cell Commitment and Differentiation. Genes. 2024; 15 (8): 1017.

39. Nunn A.D.G., Scopigno T., Pediconi N., Levrero M., Hagman H., Kiskis J., et al. The histone deacetylase inhibiting drug Entinostat induces lipid accumulation in differentiated HepaRG cells. Sci Rep. 2016; 6: 37204.
40. Tugnoli B., Bernardini C., Forni M., Piva A., Stahl C.H., Grilli E. Butyric acid induces spontaneous adipocytic differentiation of porcine bone marrow-derived mesenchymal stem cells. In Vitro Cell Dev Biol Anim. 2019; 55 (1): 17-24.
41. Stachecka J., Kolodziejski P.A., Noak M., Szczerbal I. Alteration of active and repressive histone marks during adipogenic differentiation of porcine mesenchymal stem cells. Sci Rep. 2021; 11 (1): 1325.
42. Montero-Del-Toro J.A., Serralta-Interian A.A., Nic-Can G.I., Rojas-Herrera R., Carrillo-Cocom L.M., Rodas-Junco B.A. Effect of Epigenetic Inhibitors on Adipogenesis in Human Periodontal Ligament Stem Cells. Odovtos-Int J Dent Sc. 2024; 116-128.